On Limit Cycles and the Describing Function Method in Periodically Switched Circuits

Seth R. Sanders

Abstract—**This paper begins with an examination of existence, uniqueness, and stability of limit cycles in periodically switched circuits. The motivation comes from the field of power electronics where switched circuit models composed of passive elements, independent sources, and ideal switches are studied. The paper then studies the describing function method for computation of limit cycles in these switched circuits. Typical power circuit models have nonlinear elements with characteristics that do not satisfy a Lipschitz continuity condition. As a result of these nonsmooth characteristics, previously developed justifications for the describing function method are not applicable. The present paper develops a justification for the describing function method that relies on the incrementally passive characteristics of the network elements comprising typical power electronic circuit models. This justification holds for nonsmooth circuit nonlinearities, and takes the form of a set of asymptotically convergent bounds on the errors incurred with the describing function method. In particular, the developed bounds become arbitrarily tight as the number of harmonics included in the analysis increases.**

I. Introduction

THIS PAPER begins with an examination of existence, uniqueness, and stability of limit cycles in periodically switched circuits. The motivation for this investigation comes from the field of power electronics where switched circuit models composed of passive elements, independent sources, and switches are studied. The results reported on properties of limit cycles in these switched circuits are related to analogous properties of equilibrium points in nonswitched circuits. Note that nonunique limit cycle and/or chaotic behavior may be undesirable in power electronic circuits, and these phenomena have attracted some attention recently [1]–[3].

The paper then addresses computational methods for approximating limit cycles. In particular, the paper studies the describing function method for analysis of limit cycles in periodically switched circuits. Typical power circuit models have nonlinear elements with characteristics that do not satisfy a Lipschitz continuity condition. As a result, classical averaging theory [4]–[6] is not generally applicable to these switched systems. Furthermore, the elegant justification for the describing function method given by Bergen and Franks [7] is not applicable. The results developed in the above-mentioned references are based on Lipschitz conditions on system nonlinearities. In contrast, the present paper develops a justification for the describing function method that relies on the incrementally passive characteristics of the network element comprising typical power electronic circuits. No smoothness conditions are needed. The developed justification for the describing function method takes the form of a set of asymptotically convergent bounds on the errors incurred with the method. In particular, the developed bounds become arbitrarily tight as the number of harmonics included in the analysis increases.

There is a large and growing body of literature on averaging, describing function, and related analysis techniques for power electronic circuits. See, for example [8]–[14] and also [15]–[19] for results on synthesis of averaged circuits that are realizations of the averaged state-space equations. The results reported here offer a partial justification for the generalized averaging method developed in [11].

Manuscript received December 9, 1992; revised April 26, 1993. This paper was recommended by Associate Editor J. Choma, Jr.

The author is with the Department of Electrical Engineering and Computer Sciences, University of California, Berkeley, CA 94720.

IEEE Log Number 9210967.

II. Existence, Uniqueness, and Stability of Limit Cycles

The results in this section can be considered as analogs of results for time-invariant resistive networks composed of strictly incrementally passive elements and independent sources, and as analogs of results for time-invariant dynamical circuits composed of strictly incrementally passive resistors, independent sources, and locally passive reactive elements. An *incrementally passive* multiport resistor has a characteristic that satisfies $(v' - v'')^*(i' - i'') \geq 0$ for any two points (v', i') and (v'', i'') on its characteristic with * indicating the transpose of an associated vector. The resistor is *strictly* incrementally passive if the inequality is strict for any pair of distinct points. A *locally passive* multiport capacitor is defined by a charge-voltage relationship that satisfies $(q' - q'')^*(v' - v'') \geq 0$ for any two points (q', v') and (q'', v'') on its characteristic. The capacitor is *strictly* locally passive if the inequality is strict for any two distinct points on the characteristic. An analogous definition applies for a multiport inductor. Note that the dc circuit corresponding to a time-invariant dynamical circuit is defined as the circuit obtained by replacing all inductor branches by short circuits and all capacitor

branches by open circuits. See [20] for more details on these definitions.

For nonswitched circuits, it is known [20]–[22] that:

1. Any resistive circuit constructed from strictly incrementally passive resistive elements and independent sources possesses a unique operating point if each cutset contains at least one current-controlled resistor and each loop contains at least one voltage-controlled resistor.
2. Any time-invariant dynamical circuit has a unique equilibrium point if its dc circuit has a unique operating point.
3. Any time-invariant dynamical circuit constructed from strictly incrementally passive resistive elements, independent sources, and locally passive reactive elements has a globally asymptotically stable equilibrium if there are neither capacitor-inductor-voltage source loops nor capacitor-inductor-current source cutsets.

This section contains two main results on limit cycle existence for periodically switched circuits that generalize the results quoted above for nonswitched circuits. The first pertains to circuits containing only linear reactive elements, and applies for arbitrarily large periods. The second considers the case where nonlinear reactive elements are present in the circuit, but the result is valid only for sufficiently small periods (i.e., fast switching operation).

For the purposes here, we are interested in switched circuits that possess global normal form state equations of the form

$$\frac{d}{dt}q = -(1 - u_1 - \cdots - u_m)H_0[g(q)] - u_1 H_1[g(q)] - \cdots - u_m H_m[g(q)], \quad (1)$$

where q is the vector of inductor fluxes and capacitor charges, $g(\cdot)$ is the function that maps the inductor fluxes and capacitor charges to the inductor currents and the capacitor voltages, respectively, and the $H_k(\cdot)$ $(k = 0, 1, \ldots, m)$ are hybrid representations for the resistive portion of the circuit corresponding to each possible controlled switch configuration. The $H_k(\cdot)$ need not be smooth, and indeed, nonsmooth elements such as ideal diodes may be among the resistive elements in a circuit model. Our circuit is supposed to have $m + 1$ distinct controlled switch configurations, and the following correspondence between the variables u_k and the hybrid functions $H_k(\cdot)$:

$$\begin{aligned} H_0 &\leftrightarrow u_1 = \cdots = u_m = 0, \\ H_1 &\leftrightarrow u_1 = 1, \quad u_2 = \cdots = u_m = 0, \\ &\vdots \\ H_m &\leftrightarrow u_1 = \cdots = u_{m-1} = 0, \quad u_m = 1. \end{aligned} \quad (2)$$

2.1. Linear Reactive Elements

A first result concerns the existence, uniqueness, and stability of limit cycles in periodically switched circuits built from dc sources, strictly incrementally passive resistors, ideal switches, and *linear* passive reactive elements. The linear reactive elements are assumed to be modelled by (say for a capacitor)

$$\begin{aligned} \frac{d}{dt}q &= i, \\ v &= C^{-1}q, \end{aligned} \quad (3)$$

where C is a positive definite and symmetric matrix. The inductive elements are modelled in an analogous way. For this class of circuits, we have the following:

Theorem 2.1: Suppose that during each cycle of operation of period T, there are never inductor-current source cutsets nor capacitor-voltage source loops. Furthermore, suppose that during each cycle, there is some nonzero interval of time during which each inductor branch is in a cutset with only strictly incrementally passive resistive elements and that there is some nonzero interval of time during which each capacitor branch is in a loop with only strictly incrementally passive resistive elements. Then the periodically switched circuit possesses a unique limit cycle that is globally asymptotically stable.

Outline of Proof: First, a consequence of the exclusion of inductor-current source cutsets and of capacitor-voltage source loops is that the state equation (1) exists globally. The existence, uniqueness, and stability of a limit cycle follow by taking the *energy in the increment*,

$$V(\delta i, \delta v) = \sum_{\text{Ind.}} (1/2)(\delta i_k)^* L_k(\delta i_k) + \sum_{\text{Cap.}} (1/2)(\delta v_k)^* C_k(\delta v_k) \quad (4)$$

as an incremental Lyapunov function [23], [24]. Here, $\delta i = i' - i''$ and $\delta v = v' - v''$ are the increments between any two solution trajectories (i', v') and (i'', v''), generated from different initial conditions. Because of the second part of the hypothesis, the *energy in the increment* sampled periodically (with period T) is strictly decreasing whenever it is not identically zero. In terms of a norm defined by (4), the Poincaré map obtained by periodically sampling (with period T) the capacitor voltages and inductor currents is a contraction mapping, proving the theorem. □

Example: dc–dc Converter in Discontinuous Conduction Mode. A nontrivial application for the above result occurs in dc–dc converters operating in the discontinuous conduction mode. In particular, consider the model for an up-down converter shown in Fig. 1. Note that for the continuous conduction mode, we could omit the ideal diode from the circuit model since the inductor current remains strictly positive for all time. However, it is this diode that forces the circuit into discontinuous conduction when the load is light. Since the diode is an incrementally passive resistive element, the circuit satisfies the conditions for the theorem above and hence is guaranteed to exhibit a unique, stable limit cycle.

2.2. Nonlinear Reactive Elements

In the case where nonlinear reactive elements are present in the switched circuit, we shall require that such elements be strictly locally passive. In this case, a similar

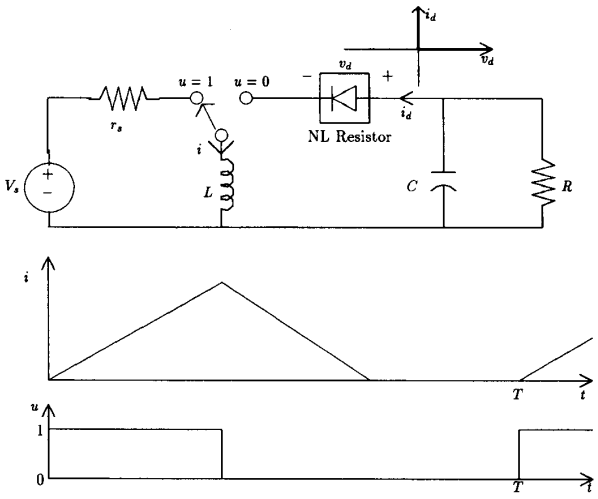

Fig. 1. Model for up-down converter in discontinuous conduction mode.

theorem holds, but only for sufficiently small periods T. It is also necessary that the right-hand side of the system equation (1) satisfy a Lipschitz condition in q and be twice differentiable with respect to q. In this case, we have the following:

Theorem 2.2: Suppose that the topological hypotheses of Theorem 2.1 hold, but nonlinear locally passive reactive elements are present in the switched circuit. Suppose also that the corresponding normal form equation (1) satisfies a Lipschitz condition in the state q and its right-hand side is twice differentiable with respect to q. Then, there exists some $T_0 > 0$ such that for all periods $T \in (0, T_0]$, the periodically switched circuit possesses a unique, asymptotically stable limit cycle.

Outline of Proof: This theorem is proved by first noting that the corresponding averaged system possesses a unique, asymptotically stable equilibrium point. Then, on an interval of length T, the solution map for the switched system can be approximated to within $O(T^2)$ by the solution map for the averaged system. Because the solution map for the periodically switched system can be obtained by continuously deforming the solution map for the averaged system, we conclude that for small enough T the two maps share the same local behavior. More details can be found in the literature on averaging theory. See, for example, [6]. □

The above results specify conditions for existence, uniqueness, and stability of limit cycles in switched circuits. The following sections analyze the describing function method for approximating a limit cycle when it is known that a circuit possesses a limit cycle.

III. The Describing Function Method

Consider the partition of a power electronic circuit into the interconnection of a reactive n-port and a resistive n-port. Suppose all reactive elements are linear and passive. In this case, the circuit can be modelled with the block diagram shown in Fig. 2. The block labelled $(Qs)^{-1}$

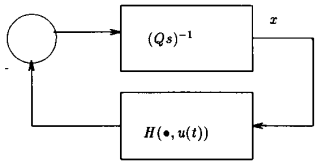

Fig. 2. Block diagrams for partitioned circuit.

is a hybrid model for the linear reactive n-port, while the block labelled $H(\cdot, u(t))$ is a hybrid model for the nonlinear switched resistive n-port. The matrix Q, which need not be diagonal, contains the inductance and capacitance values. The describing function method is based on a Fourier series representation for the state vector of the form

$$x(t) = \sum_k \langle x \rangle_k e^{jk\omega t}, \tag{5}$$

where $\omega = 2\pi/T$ corresponds to the fundamental frequency of excitation. The Fourier coefficients are determined by

$$\langle x \rangle_k = \frac{1}{T}\int_0^T x(t) e^{-jk\omega t}\, dt. \tag{6}$$

In the Fourier domain, a limit cycle is determined by the infinite set of equations that describe harmonic balance:

$$0 = -jkwQ\langle x \rangle_k + \langle H(x, u) \rangle_k \tag{7}$$

for all integers k. The quantity $\langle H(x, u) \rangle_k$ can sometimes be evaluated by consulting a table of describing functions [25]. The essence of the describing function method lies in approximating a limit cycle by truncating the infinite set of equations (7) so that only the relatively large harmonic coefficients are maintained in the calculation. The next section develops a justification for this method in the context of power electronic circuits. In particular, explicit error bounds are computed.

IV. Justification of the Describing Function Method

Suppose that in carrying out the describing function analysis, one includes terms corresponding to a certain finite subset S of the infinite set of harmonic coefficients. One would then obtain the approximation

$$\tilde{x}(t) = \sum_{k \in S} \langle \tilde{x} \rangle_k e^{jk\omega_s t} \tag{8}$$

for $x(t)$. The question addressed here is how well $\tilde{x}(t)$ approximates $x(t)$, or more appropriately how well $\tilde{x}(t)$ approximates $Px(t)$, where the operator P is defined by

$$Px(t) = \sum_{k \in S} \langle x \rangle_k e^{jk\omega t}. \tag{9}$$

Note that $P(\cdot)$ projects a periodic waveform onto the harmonic components determined by $k \in S$. The remainder of this development is aimed at determining bounds

on $\tilde{x}(t) - Px(t)$ and on $\bar{P}x(t)$, where $\bar{P}(\cdot) = I - P(\cdot)$. The approach for this follows the method of Bergen and Franks [7] and Mees [26], [27], where a system is split into two subsystems: one that governs the behavior of the fundamental coefficients used to construct $Px(t)$, and one that governs the behavior of the parasitic coefficients which result in the waveform $\bar{P}x(t)$.

Consider a circuit built from ideal sources, incrementally passive resistive elements, ideal switches, and linear passive reactive elements. Partition the circuit as shown in Fig. 2, where the reactive elements are extracted from the circuit. Associated with each reactive element is some intrinsic damping. This damping, which is typically a result of the physical nature of the element, guarantees that the linear reactive block has finite gain. No assumption of finite incremental gain is needed for the nonlinear block. Given the partition described here, the system is modelled as the feedback interconnection of a block with transfer function $G(s) = [Q(s + \alpha)]^{-1}$ and a memoryless nonlinearity described by $H(\cdot, u(t))$ which corresponds to the hybrid description of the multiport network obtained after extracting the damped reactive elements. This hybrid model is guaranteed to exist if the circuit has a well defined state-space model. Note that the linear reactive subnetwork has finite gain and is incrementally passive, while the nonlinear subnetwork is incrementally passive since it results from the interconnection of incrementally passive circuit elements. See [20] and [28] for a more detailed discussion of passivity properties of nonlinear circuits.

The system waveforms can be split into fundamental and parasitic components. The modified block diagram of Fig. 3 models the behavior of the parasitic components of the system waveforms $\bar{P}x(t)$ with the viewpoint that the fundamental components are parameters. The purpose of this description is to study the dependence of the parasitic components on the fundamental components. It can easily be seen that the operator $\bar{P}[Q(jk\omega + \alpha)]^{-1}$ in the diagram is incrementally passive and has finite gain since the corresponding element in Figure 2 has these properties. Furthermore, the gain of this element is reduced as more coefficients are included in the fundamental set because of the low pass nature of $[Q(s + \alpha)]^{-1}$. Suppose the gain (induced norm) of this element is γ. (Here, $\{x, y\} = (1/T)\int_0^T x^*(t)y(t)\,dt$ with * indicating the conjugate transpose, $\|x\| = \sqrt{\{x, x\}}$, and induced norms are defined with respect to the norm $\|\cdot\|$.) It is also true that the operator H_2 is incrementally passive as a result of the property of the analogous operator of Fig. 2. Suppose that H_2 satisfies the additional condition

$$\{H_2x - H_2x', x - x'\} \geq \epsilon\|H_2x - H_2x'\|^2 \qquad (10)$$

with real $\epsilon > 0$. The condition (10) is equivalent to a strict incremental passivity condition on H_2^{-1}, if this inverse exists. This condition is not very restrictive, as exhibited by the examples in Section 5. Given these conditions, we can apply a version of the incremental passivity theorem

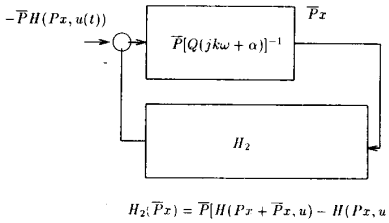

Fig. 3. Block diagram for behavior of parasitic components with fundamental components as parameters.

[28]. This theorem is reproduced with proof in the Appendix. We obtain

$$\|\bar{P}x\| \leq \gamma\left(2 + \frac{\gamma}{\epsilon}\right)\|\bar{P}H(Px, u(t))\|. \qquad (11)$$

This gives an explicit bound on the magnitude of the parasitic terms in $x(t)$ in terms of the harmonics generated by the nonlinearity $H(\cdot, u(t))$ operating on the fundamental components. Note that the bound is obtained through passivity properties, whereas previous work (such as that in [7]) developed similar bounds through a small gain argument. In our problem, the small gain theorem cannot be applied since nonlinear elements that are not Lipschitz continuous may be present.

Next consider the two block diagrams of Fig. 4. Another application of the passivity theorem allows us to generate a bound on the error in the fundamental terms incurred by ignoring the parasitic terms. In this case, the theorem is applied to generate a bound on the difference between the signals Px and $P\tilde{x}$ in the two block diagrams. We obtain

$$\|Px - P\tilde{x}\| \leq \frac{\gamma_0}{\epsilon}\|\bar{P}x\|, \qquad (12)$$

where γ_0 is the gain of the operator $P[Q(jk\omega + \alpha)]^{-1}$. Note that if $\bar{P}x$ comprises the exact parasitic terms, then $Px - P\tilde{x}$ is precisely the error incurred in the fundamental terms by using the describing function model.

By combinding (11) and (12), we obtain

$$\|Px - P\tilde{x}\| \leq \frac{\gamma_0\gamma}{\epsilon}\left(2 + \frac{\gamma}{\epsilon}\right)\|\bar{P}H(Px, u(t))\|. \qquad (13)$$

This is a bound on the error in the fundamental components incurred by using the describing function model, in terms of the harmonics generated by the actual terms. One can argue from this calculation that the approximation error in (13) decreases as more harmonic components are included in the describing function analysis, that is, as more harmonic components are viewed as fundamental components. The reasons for this are (i) the gain γ of the linear block applied to the parasitic harmonics decreases as the number of fundamental harmonics increases, and (ii) the complementary projection operator $\bar{P}$ projects onto lower dimensional subspaces as the number of fundamental harmonics increases.

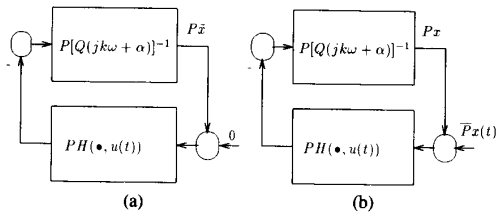

Fig. 4. (a) Block diagram for "describing function model" that ignores parasitic terms, and (b) Block diagram for fundamental components with parasitic terms as perturbation.

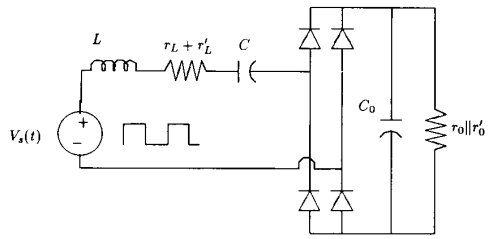

Fig. 5. Model for a series resonant converter.

The bounds (11) and (13) can be presented in a potentially more convenient form provided the absolute gain of $H(\cdot, u(t))$ is bounded, i.e., provided

$$\| H(x, u(t)) \| \leq k_1 \| x \| + k_2 \tag{14}$$

and, hence,

$$\| \bar{P}H(Px, u(t)) \| \leq k_1 \| Px \| + k_2 \tag{15}$$

for some nonnegative real constants k_1 and k_2. This condition does not require that $H(\cdot, u(t))$ have finite incremental gain. Then, one obtains

$$\| \bar{P}H(Px, u(t)) \| \leq k_1 \| Px - P\tilde{x} \| + k_1 \| P\tilde{x} \| + k_2 \tag{16}$$

by the triangle inequality. Combining this relationship with (13), one finds

$$\| Px - P\tilde{x} \| \leq \frac{\gamma_0 \gamma}{\epsilon} \left(2 + \frac{\gamma}{\epsilon} \right) \left(k_1 \| Px - P\tilde{x} \| + k_1 \| P\tilde{x} \| + k_2 \right). \tag{17}$$

Then, if the quantity $\delta = (\gamma_0 \gamma / \epsilon)(2 + \gamma/\epsilon) k_1$ is less than 1, one finally obtains

$$\| Px - P\tilde{x} \| \leq \frac{\delta}{1 - \delta} \left(\| P\tilde{x} \| + \frac{k_2}{k_1} \right). \tag{18}$$

Note that the quantity δ can always be made less than 1 by including a sufficient number of harmonic components in the fundamental set because of the low pass nature of the linear reactive subnetwork. By combining (11), (16), and (18), one can write

$$\| \bar{P}x \| \leq \gamma \left(2 + \frac{\gamma}{\epsilon} \right) \frac{1}{1 - \delta} (k_1 \| P\tilde{x} \| + k_2). \tag{19}$$

The results (18) and (19) are quite convenient since these results give bounds on the error incurred with the describing function method in terms of quantities computed with the describing function method. Note that all bounds developed here are asymptotically convergent since these bounds become arbitrarily tight as the number of harmonics included in the describing function analysis increases. See the examples below for details on the application.

V. Examples

5.1. Series Resonant Converter

To illustrate the application of the theory developed in the previous section, we first consider the simplified model of the series resonant converter of Fig. 5. In practice, the square-wave drive is developed with a half-bridge or full-bridge circuit. This circuit is usually operated with the switching frequency (frequency of the driving square wave) just above or just below the resonant frequency of the L-C network. Here, let us consider the case where the circuit is operated above resonance, which permits zero-voltage switching operation for the power switches and diodes [29].

The first step is to partition the circuit into a linear reactive two-port and a nonlinear, time-varying resistive two-port as shown in Fig. 6. The linear reactive two-port network consists of the damped L-C network and the damped output filter capacitor. Note that we have divided the series resistance $r_L + r'_L$ into a damping term r_L associated with the resonant tank and a term r'_L associated with the nonlinear resistive network. A similar step has been taken with the output load resistor. We have also lumped the resonant L-R-C network into a single port, rather than complicate the analysis by including a port for each of the reactive elements. With the indicated partition, the linear reactive network is described by

$$\begin{bmatrix} -i_1 \sqrt{R_1} \\ v_2 / \sqrt{R_2} \end{bmatrix} = \begin{bmatrix} \dfrac{sCR_1}{s^2 LC + sr_L C + 1} & 0 \\ 0 & \dfrac{r_0 / R_2}{sC_0 r_0 + 1} \end{bmatrix} \cdot \begin{bmatrix} v_1 / \sqrt{R_1} \\ -i_2 \sqrt{R_2} \end{bmatrix}, \tag{20}$$

where $\sqrt{R_1}$ and $\sqrt{R_2}$ are scaling factors that may be picked to facilitate the analysis. The scaling factors are needed to give meaning to the various constants that are to be calculated. We obtain immediately that

$$\gamma_0 \leq \max (R_1 / r_L, r_0 / R_2). \tag{21}$$

The nonlinear resistive network is described by

$$\begin{bmatrix} v_1 / \sqrt{R_1} \\ i_2 \sqrt{R_2} \end{bmatrix} = \begin{bmatrix} r'_L / R_1 & \sqrt{R_2 / R_1}\, \operatorname{sgn}(i_1) \\ -\sqrt{R_2 / R_1}\, \operatorname{sgn}(i_1) & R_2 / r'_0 \end{bmatrix} \cdot \begin{bmatrix} i_1 \sqrt{R_1} \\ v_2 / \sqrt{R_2} \end{bmatrix} + \begin{bmatrix} -V_s(t) / \sqrt{R_1} \\ 0 \end{bmatrix}, \tag{22}$$

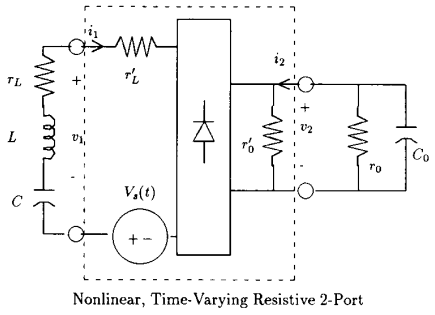

Fig. 6. Partition of series resonant converter.

where $\operatorname{sgn}(\cdot)$ is the sign function, defined by

$$\operatorname{sgn}(x) = \begin{cases} 1, & x \geq 0, \\ -1, & x < 0. \end{cases} \tag{23}$$

It turns out that for this particular nonlinear hybrid model, it is possible to compute its inverse and consequently to obtain the constant ϵ. Recall that ϵ is a measure of the incremental lossyness of the nonlinear resistive network. In particular, we compute

$$\epsilon = \frac{\min(R_2/r'_0, r'_L/R_1)}{(R_2/R_1)(1 + r'_L/r'_0)}. \tag{24}$$

Note that it is possible to pick R_1, R_2, and the ratios r_L/r'_L and r'_0/r_0 to make the resulting bounds as tight as possible. For the purposes here, we shall make rather arbitrary choices for these parameters to simplify the calculations. We take

$$R_2 = r'_0, \tag{25}$$

$$R_1 = r'_L, \tag{26}$$

$$r'_0 = r_0, \tag{27}$$

$$r'_L = r_L. \tag{28}$$

We immediately obtain $\gamma_0 = 1$. In a realistic design that attains a reasonable level of power efficiency, it must be true that $r_0 \gg r_L$. Let us assume $r_0 = 9r_L$ which then yields $\epsilon = 0.1$. The gain parameter γ depends upon how many harmonic coefficients are included as fundamental components in the describing function analysis. If we include the DC and first harmonic terms, we obtain the estimate $\gamma \approx 0.01$. The rationale for this estimate is that at the frequency of the second harmonic ($\omega \approx 2/\sqrt{LC}$), the admittance of the L-R-C network is controlled approximately by a one-pole roll-off and the impedance of the R-C network is also controlled by a one-pole roll-off. For the L-R-C network, we estimate the scaled admittance as $\frac{1}{2}(r_L/\sqrt{L/C})$. If the quality factor Q of this resonant network is on the order of 50 (which is reasonable), we find the scaled admittance of this element to be approximately 0.01. For the R-C network at the output, the scaled impedance will have a magnitude of approximately 0.01 at the second harmonic frequency if the time constant r_0C_0 is 50 times $\sqrt{LC}$. This corresponds to a reasonable design with respect to output ripple voltage.

With this information, we are in a position to calculate various bounds. The bound corresponding to (11) takes the form

$$\|\bar{P}x\| \leq 0.0201 \|\bar{P}H(Px, u(t))\|. \tag{29}$$

Noting that it is possible to calculate the bound $\|\bar{P}H(Px, u(t))\| \leq 2.31\|Px\| + 0.434\|V_s(t)/\sqrt{R_1}\|$ on harmonics generated by this particular circuit nonlinearity, we obtain the bound

$$\|\bar{P}x\| \leq 0.046\|Px\| + 0.0086\left\|\frac{V_s(t)}{\sqrt{R_1}}\right\|. \tag{30}$$

This is an explicit bound on the parasitic harmonic terms in terms of the actual fundamental harmonics. Such a tight bound is indicative that the describing function method is useful for this problem. Next, the bound corresponding to (13) takes the form

$$\|Px - P\tilde{x}\| \leq 0.201 \|\bar{P}H(Px, u(t))\|. \tag{31}$$

Again, combining with $\|\bar{P}H(Px, u(t))\| \leq 2.31\|Px\| + 0.434\|V_s(t)/\sqrt{R_1}\|$, the bound

$$\|Px - P\tilde{x}\| \leq 0.46\|Px\| + 0.086\left\|\frac{V_s(t)}{\sqrt{R_1}}\right\| \tag{32}$$

is obtained. This is an explicit bound on the error in the fundamental terms computed with the describing function method. This bound is computed with respect to the fundamental harmonics of the actual circuit waveforms.

It is also possible to invoke the triangle inequality $\|Px\| \leq \|P\tilde{x}\| + \|Px - P\tilde{x}\|$ to obtain bounds on the above quantities in terms of the approximate circuit waveforms computed with the describing function method. In particular, the corresponding bounds that result are

$$\|\bar{P}x\| \leq 0.1\|P\tilde{x}\| + 0.04\left\|\frac{V_s(t)}{\sqrt{R_1}}\right\| \tag{33}$$

and

$$\|Px - P\tilde{x}\| \leq 0.85\|P\tilde{x}\| + 0.18\left\|\frac{V_s(t)}{\sqrt{R_1}}\right\|. \tag{34}$$

The latter are especially interesting since one only needs to make calculations with the describing function technique in order to obtain these bounds.

Note that all calculated bounds become tighter as additional harmonics are included in the analysis, that is, as additional harmonics are included in the fundamental set. The following example illustrates this feature.

5.2. *Pulse-Width Modulated Up-Down Converter*

The second example to be studied is the pulse-width modulated up-down converter of Fig. 7. The calculations presented here apply for the continuous conduction mode. The analysis could be modified to include the discontinu-

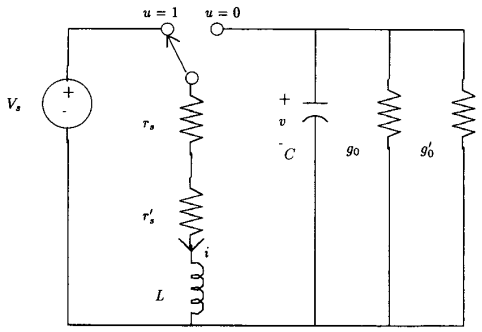

Fig. 7. Up-down converter model.

ous conduction mode, as well, but with some additional complication. This circuit is usually designed so that the ripple in the inductor current and the output capacitor voltage are small fractions of their respective dc values. The circuit has traditionally been analyzed with the state-space averaging procedure [8], [9]. Our analysis provides a bound on the energy in the ripple and a bound on the error in the dc component when dc equilibrium analysis of the so-called state-space averaged model [8] is carried out. This is precisely describing function analysis with only the dc component. In the case where dc and certain principle harmonics are included in the describing function calculations, our analysis provides a bound on the energy in the residual (ignored harmonics) of the ripple waveforms and a bound on the energy in the error in the dc and principle harmonics computed with the descricing function method.

The first step is to partition the circuit into a linear reactive two-port and a time-varying resistive two-port as shown in Fig. 8. In this example, the resistive two-port is linear, but time-varying. As in the previous example, the series resistance $r_s + r'_s$ associated with the inductor (and possibly the power switches) is split into two terms, namely, a damping term r_s associated with the inductor and a term r'_s associated with the switch network. A similar step is taken with the load resistance. With this partition, the linear two-port is modelled by

$$\begin{bmatrix} -i_1\sqrt{R_1} \\ v_w/\sqrt{R_2} \end{bmatrix} = \begin{bmatrix} \dfrac{R_1}{r_s + sL} & 0 \\ 0 & \dfrac{1}{R_2(sC + g_0)} \end{bmatrix} \begin{bmatrix} v_1/\sqrt{R_1} \\ -i_2\sqrt{R_2} \end{bmatrix}, \tag{35}$$

where $\sqrt{R_1}$ and $\sqrt{R_2}$ are scaling factors. We find

$$\gamma_0 \le \max\left(\frac{R_1}{r_s}, \frac{1}{R_2 g_0}\right). \tag{36}$$

The switched resistive two-port is modelled by

$$\begin{bmatrix} v_1/\sqrt{R_1} \\ i_2\sqrt{R_2} \end{bmatrix} = \begin{bmatrix} r'_s/R_1 & \sqrt{R_2/R_1}\,(1-u) \\ -\sqrt{R_2/R_1}\,(1-u) & g'_0 R_2 \end{bmatrix} \cdot \begin{bmatrix} i_1\sqrt{R_1} \\ v_2/\sqrt{R_2} \end{bmatrix} + \begin{bmatrix} uV_s/\sqrt{R_1} \\ 0 \end{bmatrix}, \tag{37}$$

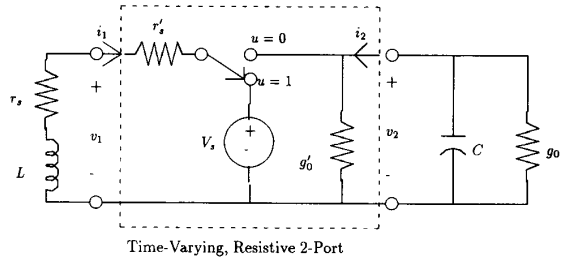

Fig. 8. Partion of up-down converter.

where u is an indicator of switch position as shown in Figs. 7 and 8. For this particular switched two-port, it is possible to compute ϵ, the measure of incremental lossyness. We find

$$\epsilon = \frac{\min(r'_s/R_1, g'_0 R_2)}{(R_2/R_1)(1 + r'_s g'_0)}. \tag{38}$$

It is possible to pick R_1, R_2, and the ratios r_s/r'_s and g'_0/g_0 to make our bounds as tight as possible. Here, we make the convenient choices

$$R_1 = r'_s, \tag{39}$$

$$r_s = r'_s, \tag{40}$$

$$R_2 = 1/g'_0, \tag{41}$$

$$g_0 = g'_0. \tag{42}$$

A result of the above selection is that $\gamma_0 = 1$. Any design that attains a useful level of power efficiency must have $r_s \ll 1/g_0$. Assuming $r_s = 1/(9g_0)$, we find $\epsilon = 0.1$. The gain parameter γ depends upon how many harmonics are included in the describing function analysis. If we include only dc terms, that is, the analysis corresponds to equilibrium computation with an averaged model, we estimate $\gamma \approx 0.02$. The rationale for this estimate is that at the frequency of the first harmonic (the switching frequency), a typical circuit will satisfy $|j\omega_s L| > 50r_s$ and $|j\omega_s C| > 50g_0$. If the first N harmonics are included in the analysis, then we would estimate $\gamma \approx 0.02/(N+1)$.

Now, we can calculate various bounds of interest. If only the dc component is included in our analysis, the bound corresponding to (11) takes the form

$$\|\bar{P}x\| \le 0.044\|\bar{P}H(Px, u(t))\|. \tag{43}$$

For the hybrid model (37) of the switched two-port network, it is possible to compute the bound

$$\|\bar{P}H(Px, u(t))\| \le 1.5\|Px\| + 0.5\left\|\frac{V_s}{\sqrt{R_1}}\right\| \tag{44}$$

on the harmonics it generates by operating on the fundamental (dc) term. Combining these inequalities generates the explicit bound

$$\|\bar{P}H(Px, u(t))\| \leq 0.066\|Px\| + 0.022\left\|\frac{V_s}{\sqrt{R_1}}\right\| \quad (45)$$

on the energy in the ripple waveforms expressed in terms of the dc components of the actual circuit waveforms. Once again, the tightness of the bound indicates that the describing function method (or simply averaging in this case) will be effective. The bound corresponding to (13) on the error in the computed dc term takes the form

$$\|Px - P\tilde{x}\| \leq 0.44\|\bar{P}H(Px, u(t))\|. \quad (46)$$

Combining with (44) yields

$$\|Px - P\tilde{x}\| \leq 0.66\|Px\| + 0.22\left\|\frac{V_s}{\sqrt{R_1}}\right\|, \quad (47)$$

which is a bound on the error in the computed dc terms expressed in terms of the actual circuit dc terms.

One would expect the describing function method to yield improved results as additional harmonics are included in the analysis, and this is made evident by the bounds computed below for this example. If the dc and first N harmonic terms are included in the describing function analysis, then the bound corresponding to (11) takes the form

$$\|\bar{P}x\| \leq \frac{0.02}{N+1}\left(2 + \frac{0.2}{N+1}\right)\|\bar{P}H(Px, u(t))\|. \quad (48)$$

Combining with the bound (44), which is still valid, but not tight, we obtain

$$\|\bar{P}x\| \leq \frac{0.03}{N+1}\left(2 + \frac{0.2}{N+1}\right)\|Px\| + \frac{0.01}{N+1}\left(2 + \frac{0.2}{N+1}\right)\left\|\frac{V_s}{\sqrt{R_1}}\right\|. \quad (49)$$

This is a general formula for an asymptotically convergent bound on the harmonics generated by the fundamental components of the actual circuit waveforms. With the dc and first N harmonics included in the analysis, the bound corresponding to (13) takes the form

$$\|Px - P\tilde{x}\| \leq \frac{0.2}{N+1}\left(2 + \frac{0.2}{N+1}\right)\|\bar{P}H(Px, u(t))\|. \quad (50)$$

Combining with (44), we obtain

$$\|Px - P\tilde{x}\| \leq \frac{0.3}{N=1}\left(2 + \frac{0.2}{N+1}\right)\|Px\| + \frac{0.1}{N+1}\left(2 + \frac{0.2}{N+1}\right)\left\|\frac{V_s}{\sqrt{R_1}}\right\|, \quad (51)$$

which is an asymptotically convergent bound on the energy in the error in the fundamental components as computed with the describing function method. This bound is expressed in terms of the fundamental components of the actual circuit waveforms.

VI. Conclusion

After establishing conditions for the existence, uniqueness, and stability of a limit cycle in a periodically switched circuit, this paper offers a justification for the use of the describing function method for computation of the limit cycle. In contrast to previous work, nonlinear elements that do not satisfy a Lipschitz condition can be included in the analysis. The analysis presented here generates explicit bounds on the error incurred with the describing function method. The bounds are shown to become arbitrarily tight as the number of harmonics included in the analysis increases.

A. Appendix
Incremental Passivity Theorem

Theorem A.1 (Incremental Passivity Theorem): Suppose that the operator labelled H_1 in Fig. 9 has finite incremental gain γ and is incrementally passive. Suppose that H_2 is incrementally passive and satisfies $\{H_2x - H_2x', x - x'\} \geq \epsilon\|H_2x - H_2x'\|^2$ for $\epsilon > 0$, i.e., H_2^{-1} is strictly incrementally passive if it exists. Then, (i) for any inputs u_1 and u_2 with bounded norm, the outputs e_1, e_2, y_1, y_2 are unique and have bounded norms, and (ii) the mapping $(u_1, u_2) \to (e_1, e_2, y_1, y_2)$ has bounded gain.

The proof of this theorem is modified from a very similar proof in [28]. The important part of the proof that establishes uniqueness also generates the bounds used in Section 4. In particular, by considering two sets of inputs (u_1, u_2) and (u_1', u_2'), we obtain

$$\{e_1 - e_1', H_1e_1 - H_1e_1'\} + \{e_2 - e_2', H_2e_2 - H_2e_2'\} = \{u_1 - u_1', H_1e_1 - H_1e_1'\} + \{u_2 - u_2', H_2e_2 - H_2e_2'\}. \quad (52)$$

Then by invoking the incremental passivity properties and the bound on H_1, we find

$$\epsilon\|H_2e_2 - H_2e_2'\|^2 \leq \gamma\|u_1 - u_1'\| \cdot \|e_1 - e_1'\| + \|u_2 - u_2'\| \cdot \|e_1 - e_1'\| + \|u_1 - u_1'\| \cdot \|u_2 - u_2'\|. \quad (53)$$

From the block diagrams, we find

$$\epsilon\|u_1 - u_1'\|^2 - 2\epsilon\|u_1 - u_1'\| \cdot \|e_1 - e_1'\| + \epsilon\|e_1 - e_1'\|^2 \leq \gamma\|u_1 - u_1'\| \cdot \|e_1 - e_1'\| + \|u_2 - u_2'\| \cdot \|e_1 - e_1'\| + \|u_1 - u_1'\| \cdot \|u_2 - u_2'\|, \quad (54)$$

which leads to

$$\epsilon\|e_1 - e_1'\|^2 \leq (2\epsilon + \gamma)\|u_1 - u_1'\| \cdot \|e_1 - e_1'\| + \|u_2 - u_2'\| \cdot \|e_1 - e_1'\| + \|u_2 - u_2'\| \cdot \|u_1 - u_1'\|. \quad (55)$$

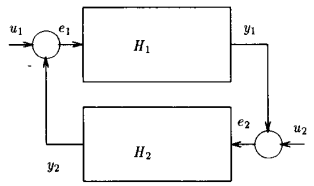

Fig. 9. Feedback system.

By considering the case where $u_1 = u_1'$, we obtain the bounds

$$\|e_1 - e_1'\| \le 1/\epsilon \|u_2 - u_2'\|, \tag{56}$$

$$\|e_2 - e_2'\| \le \frac{\gamma}{\epsilon}\|u_2 - u_2'\|. \tag{57}$$

By considering the case where $u_2 = u_2'$, we obtain the bounds

$$\|e_1 - e_1'\| \le \left(2 + \frac{\gamma}{\epsilon}\right)\|u_1 - u_1'\|, \tag{58}$$

$$\|e_2 - e_2'\| \le \gamma\left(2 + \frac{\gamma}{\epsilon}\right)\|u_1 - u_1'\|. \tag{59}$$

These are the relationships used in Section 4.

References

[1] J. B Deane and D. C. Hamill, "Analysis, simulation, and experimental study of chaos in the buck converter," *IEEE PESC Record*, 1990, pp. 491–498.

[2] J. H. B. Deane and D. C. Hamill, "Instability, subharmonics, and chaos in power electronic systems,' *IEEE PESC Record*, 1989, pp. 34–42.

[3] P. T. Krein and R. M. Bass, "Multiple limit cycle phenomena in switching power converters," *IEEE Applied Power Electronics Conf.*, 1989, pp. 143–148.

[4] N. N. Bogoliubov and Y. A. Mitropolsky, *Asymptotic Methods in the Theory of Nonlinear Oscillations*. Delhi, India: Hindustan Publishing Corp., 1961.

[5] J. A. Sanders and F. Verhulst, *Averaging Methods in Nonlinear Dynamical Systems*. New York: Springer-Verlag, 1985.

[6] J. Guckenheimer and P. Holmes, *Nonlinear Oscillations, Dynamical Systems, and Bifurcations of Vector Fields*. New York: Springer-Verlag, 1983.

[7] A. R. Bergen and R. L. Franks, "Justification of the describing function method," *SIAM J. Control*, vol. 9, no. 4, Nov. 1971.

[8] R. D. Middlebrook and S. Cuk, "A general unified approach to modeling switching power converter stages," *IEEE PESC Record*, 1976, pp. 18–34.

[9] R. W. Brockett and J. R. Wood, "Electrical networks containing controlled switches," Addendum to *IEEE Symposium on Circuit Theory*, April 1974.

[10] P. T. Krein, J. Bentsman, R. M. Bass, and B. C. Lesieutre, "On the use of averaging for the analysis of power electronic systems," *IEEE Trans. Power Electron*, vol. PE-5, no. 2, pp. 182–190, April 1990.

[11] S. R. Sanders, J. M. Noworolski, X. Z. Liu, and G. C. Verghese, "Generalized averaging method for power conversion circuits," *IEEE Trans. Power Electron*, vol. PE-6, no. 2, April 1991.

[12] R. L. Steigerwald, "A comparison of half-bridge resonant converter topologies," *IEEE Trans. Power Electron.*, vol. PE-3, no. 2, pp. 174–182, April 1988.

[13] M. K. Kazimierczuk and S. Wang, "Frequency-domain analysis of series resonant converter for continuous conduction mode," *IEEE Trans. Power Electron.*, vol. PE-7, no. 2, pp. 270–279, April 1992.

[14] A. Kislovski, R. Redl, and N. O. Sokal, *Analysis of Switching-Mode DC/DC Converters*. New York: Van Nostrand, 1991.

[15] S. R. Sanders and G. C. Verghese, "Synthesis of averaged circuit models for switched power converters," *IEEE Trans. Circuits Syst.*, vol. CAS-38, no. 8, pp. 905–915, Aug. 1991.

[16] J. M. Noworolski and S. R. Sanders, "Generalized in-place circuit averaging," *IEEE Applied Power Electronics Conference*, March 1991, Dallas, pp. 445–451.

[17] V. Vorperian, "Simplify your PWM converter analysis using the model of the PWM switch, Part I: Continuous conduction mode," *Current* (Virginia Polytech Newsletter), Fall 1988, pp. 8–13; "Part II: Discontinuous conduction mode," *Current*, Spring 1989, pp. 6–12.

[18] G. W. Wester and R. D. Middlebrook, "Low frequency characterization of switched DC-DC converters," *IEEE PESC Record*, 1972.

[19] D. Dzarkowski and M. K. Kazimierczuk, "Linear circuit models of PWM flyback and buck/boost converters," *IEEE Trans. Circuits Syst.*, vol. CAS-39, no. 8, pp. 688–693, Aug. 1992.

[20] M. Hasler and J. Neirynck, *Nonlinear Circuits*. Artech House, 1986.

[21] L. O. Chua, Course notes for EECS 223, Dept. EECS, UC Berkeley, 1980.

[22] C. A. Desoer and F. F. Wu, "Nonlinear monotone networks," *SIAM J. Appl. Math.*, vol. 26, no. 2, pp. 315–333, March 1974.

[23] L. O. Chua and D. N. Green, "A qualitative analysis of the behavior of dynamic nonlinear networks: Steady-state solutions of nonautonomous networks," *IEEE Trans. Circuits Syst.*, vol. CAS-23, no. 9, pp. 530–550, Sept. 1976.

[24] S. R. Sanders, "Nonlinear control of switching power converters," PhD Thesis, Dept. EECS, MIT, 1989.

[25] A. Gelb and W. E. Vander Velde, *Multiple-Input Describing Functions and Nonlinear System Design*. New York: McGraw-Hill Book Co., 1968.

[26] A. I. Mees, "The describing function matrix," *J. Inst. Math. Appl.*, vol. 10, pp. 49–67, 1972.

[27] A. I. Mees, "Limit cycle stability," *J. Inst. Math. Appl.*, vol. 11, pp. 281–295, 1973.

[28] C. A. Desoer and M. Vidyasagar, *Feedback Systems: Input-Output Properties*. New York: Academic Press, 1975.

[29] J. Kassakian, M. Schlecht, and G. Verghese, *Principles of Power Electronics*. Reading, MA: Addison-Wesley, 1991.

Seth R. Sanders received S.B. degrees in electrical engineering and physics from MIT Cambridge, MA in 1981. He then worked as a design engineer at the Honeywell Test Instrument Division in Denver, CO. He returned to MIT in 1983 and received the S.M. and Ph.D. degrees in electrical engineering in 1985 and 1989, respectively.

He is presently an assistant professor in the Department of Electrical Engineering and Computer Sciences at the University of California, Berkeley. His research interests are in nonlinear circuits and systems, and particularly in applications to power electronic and electromechanical systems. During the 1992–1993 academic year, he was on industrial leave with National Semiconductor in Santa Clara, CA.